OPEN ACCESS

ORIGINAL ARTICLE

Role of TLR4 in the gut-brain axis in Parkinson's disease: a translational study from men to mice

Paula Perez-Pardo,[1] Hemraj B Dodiya,[2] Phillip A Engen,[2] Christopher B Forsyth,[2] Andrea M Huschens,[1] Maliha Shaikh,[2] Robin M Voigt,[2] Ankur Naqib,[3] Stefan J Green,[3,4] Jeffrey H Kordower,[5] Kathleen M Shannon,[5] Johan Garssen,[1,6] Aletta D Kraneveld,[1,7] Ali Keshavarzian[1,2]

► Additional material is published online only. To view, please visit the journal online (http://dx.doi.org/10.1136/gutjnl-2018-316844).

For numbered affiliations see end of article.

Correspondence to
Dr Paula Perez-Pardo, Universiteit Utrecht, Utrecht 3584CG, The Netherlands; p.perezpardo@uu.nl

PP-P and HBD contributed equally.
ADK and AK contributed equally.

Received 22 May 2018
Revised 27 November 2018
Accepted 27 November 2018
Published Online First
15 December 2018

ABSTRACT

Objective Recent evidence suggesting an important role of gut-derived inflammation in brain disorders has opened up new directions to explore the possible role of the gut-brain axis in neurodegenerative diseases. Given the prominence of dysbiosis and colonic dysfunction in patients with Parkinson's disease (PD), we propose that toll-like receptor 4 (TLR4)-mediated intestinal dysfunction could contribute to intestinal and central inflammation in PD-related neurodegeneration.

Design To test this hypothesis we performed studies in both human tissue and a murine model of PD. Inflammation, immune activation and microbiota composition were measured in colonic samples from subjects with PD and healthy controls subjects and rotenone or vehicle-treated mice. To further assess the role of the TLR4 signalling in PD-induced neuroinflammation, we used TLR4-knockout (KO) mice in conjunction with oral rotenone administration to model PD.

Results Patients with PD have intestinal barrier disruption, enhanced markers of microbial translocation and higher pro-inflammatory gene profiles in the colonic biopsy samples compared with controls. In this regard, we found increased expression of the bacterial endotoxin-specific ligand TLR4, CD3+ T cells, cytokine expression in colonic biopsies, dysbiosis characterised by a decrease abundance of SCFA-producing colonic bacteria in subjects with PD. Rotenone treatment in TLR4-KO mice revealed less intestinal inflammation, intestinal and motor dysfunction, neuroinflammation and neurodegeneration, relative to rotenone-treated wild-type animals despite the presence of dysbiotic microbiota in TLR4-KO mice.

Conclusion Taken together, these studies suggest that TLR4-mediated inflammation plays an important role in intestinal and/or brain inflammation, which may be one of the key factors leading to neurodegeneration in PD.

Significance of this study

What is already known on this subject?

- Parkinson's disease (PD) symptoms go beyond motor dysfunction since patients very often develop non-motor problems including GI dysfunctions.
- GI symptoms can begin decades before the onset of motor symptoms and are major determinants for quality of life of patients with PD.
- The intestinal tract could be a major source of inflammation contributing to neurodegeneration in PD.

What are the new findings?

- Patients with PD have an increased expression of the bacterial endotoxin-specific ligand toll-like receptor 4 (TLR4), intestinal barrier disruption, enhanced makers of bacterial translocation and higher pro-inflammatory gene profiles in the colon when compared with healthy controls.
- Rotenone treatment in TLR4-knock out mice shows less intestinal inflammation. Intestinal and motor dysfunction, brain neuroinflammation and neurodegeneration relative to rotenone-treated wild-type animals.

How might it impact on clinical practice in the foreseeable future?

- TLR4 (gut)-mediated inflammation might be involved in PD development and therefore might be an important target for future treatments of PD.
- There is a need for further investigation into the role of TLR4-mediated intestinal and neuroinflammation and gut-brain interactions in the pathogenesis of PD.

INTRODUCTION

The mechanism of neurodegeneration in Parkinson's disease (PD) remains unknown but converging evidence suggests that inflammation-derived oxidative stress and cytokine toxicity may play a critical role.[1–7] The intestinal tract could be a contributing factor to the neurodegenerative processes in PD. Intestinal dysfunctions including constipation are common in PD and can begin decades before the onset of motor symptoms. In this regard, studies by our group[8 9] and others[10–13] suggest that the intestinal tract, especially the colon and its microbiota community,[14] could be a major source of inflammation contributing to neurodegeneration.

Our group and others report that patients with PD exhibit a pro-inflammatory microbiota profile[9 12 15–17] with a reduction in beneficial products such as short chain fatty acids.[13] Reconstitution of the faecal microbiota in germ-free

Check for updates

To cite: Perez-Pardo P, Dodiya HB, Engen PA, *et al*. *Gut* 2019;**68**:829–843.

alpha-synuclein (α-syn) transgenic PD mice using stool from our patients with PD exacerbates motor symptoms and pathology in this PD model.[18] In addition, the microbiota via mechanisms including metabolite production can impact immune and inflammatory pathways leading to the peripheral and central immune activation and inflammation.[19 20] Finally, the intestinal barrier is critical to separate the pro-inflammatory contents of the intestine from the systemic circulation. Intestinal hyperpermeability is observed in patients with PD[8] and likely contributes to microbiota-initiated inflammation in PD.

Consequences of intestinal dysbiosis and/or intestinal barrier dysfunction include immune activation and inflammation. Examples include involvement of toll-like receptor (TLR) pathway activations and abnormal immune activations such as CD3 T cells. Increased T-cell trafficking into the colonic mucosa is a feature associated with constipated patients with PD.[21] In addition, activation of various TLRs, specifically TLR4 is of interest since the Gram-negative bacteria activate this receptor. If abnormalities in the microbiome (especially favouring lipopolysaccharide (LPS) producers) are an initial trigger for PD pathogenesis in the intestinal tract, TLR4 might be the first point of microbial interaction.

There are several potential mechanisms by which intestinal inflammation and immune activation secondary to intestinal dysbiosis or intestinal barrier dysfunction might lead to central nervous system pathology. Inflammation and immune activation could initiate α-syn pathology in the enteric nervous system that then spreads in a prion-like fashion via the vagus nerve to the lower brainstem, and then the substantia (SN).[22] Our group and others have shown α-syn accumulations in colonic tissue from patients with PD prior to the onset of motor symptoms.[23–25] Alternatively, gut-derived bacterial products or the peripheral inflammatory response (eg, cytokine production) could impact the brain through systemic mechanisms including disruption of the blood-brain barrier as is observed in patients with PD.[26] Thus, chronic activation of intestinal and peripheral immune cells and pro-inflammatory cytokines could initiate or promote neurodegeneration leading to PD.

Taken together, we hypothesise that microbiota dysbiosis and gut leakiness to bacterial endotoxins activates TLR4-mediated inflammatory cascades leading to neurodegeneration in PD. To test this hypothesis, we performed studies in both human tissue and a murine model of PD. Inflammation and immune activation were measured in colonic mucosal samples from subjects with PD and healthy controls (HC) subjects and rotenone or vehicle-treated mice. To further assess the role of the TLR4 receptor, we used TLR4-knockout (KO) mice in conjunction with oral rotenone administration to model PD.

METHODS

Part I: human study

Healthy control subjects and subjects with PD

HC subjects (n=6) and non-constipated patients with PD (n=6) were recruited by Rush University Medical Center (RUMC) (Chicago, Illinois, USA) (online supplementary table S1). All subjects signed a consent form for use of their samples and data to be part of a RUMC Institutional Review Board-approved GI repository and the ongoing research. HC subjects had no history of GI or neurological disorders. Subjects with PD diagnosed by the UK Parkinson's Disease Research Society Brain Bank criteria were recruited according to a previously published protocol.[23]

Collection of colon biopsies, faecal and blood samples

Study samples were collected after overnight fast and the morning dose of levodopa was given after collection. Subjects underwent an unprepped, limited sigmoidoscopy by one of the authors (AK) and eight mucosal biopsy samples were taken from distal sigmoid colon and stool collected from each subject, as published previously[23] and described in the online supplemental material and methods. Six millilitres of blood was collected using normal aseptic techniques. Plasma was separated by centrifugation at 1500×g at 4°C for 15 min and stored at −80°C for LPS-binding protein (LBP) measurements.

Intestinal permeability and endotoxin (LBP) measurements

All subjects with PD and HC subjects followed our established protocol to measure total gut permeability.[8] All subjects fasted overnight and subsequently ingested a sugar mixture containing 2 g mannitol, 7.5 g lactulose, 40 g sucrose and 1 g sucralose. Urine samples were collected 24 hours after oral sugar probe administration and frozen in liquid nitrogen for gas chromatography analyses as established[27] to measure total excreted sugar levels. Systemic levels of bacterial endotoxin were determined using LBP measurements according to our established procedure from subjects with PD (n=5) and HC subjects (n=5).[28]

Immunocytochemistry and microscopic analyses

Immunofluorescence staining and microscopic analyses in human biopsies (n=6 subjects with PD and n=6 HC subjects) were performed to assess integrity of the tight junctional protein zonula occludens 1 (ZO-1) and TLR4 markers, as previously published[29] and described in the online supplemental material and methods.

mRNA expression analyses

Genes specific for microbiota-induced intestinal inflammation and gut dysfunction were evaluated according to a published protocol,[30] and described in the online supplemental material and methods.

Statistical analyses

All data are expressed as mean±SEM. Differences between HC and PD groups were statistically analysed with an unpaired two-tailed t-test. Correlations were performed using non-parametric analysis. Significance was selected at $p<0.05$. Analyses were performed using Graph Pad Prism V.1.5.

Part II: mice study

Animal housing

C57BL/6J wild-type (WT) and TLR4-KO mice (Jackson Laboratories) aged 7 weeks were housed under a 12-hour light/dark cycle. Food and water were provided ad libitum.

Mouse model for PD

WT and TLR4-KO mice received a rotenone (Sigma-Aldrich, The Netherlands) solution (10 mg/kg suspended freshly in 4% carboxymethylcellulose and 1.25% chloroform vehicle) once a day for 28 days by oral gavage, as described before.[31] Control animals received vehicle. On day 28, mice were sacrificed and the brain and the intestinal tissue were collected for analysis.

Motor function assessment

Motor function of mice was assessed by the Rotarod test as described before[31] and as described in the online supplemental material and methods.

Intestinal transit and colon length

Thirty minutes before sacrificing the mice, a solution of 2.5% Evans blue (Sigma-Aldrich) in 1.5% methylcellulose (0.3 mL per animal) was intragastrically administered to the mice. After euthanasia, intestinal transit was measured as the distance from the pylorus to the most distal point of migration. In addition, the length of the colon was measured.

Assessment of intestinal barrier integrity

We elected to assess integrity of tight junctional protein in the colon of our mice as a marker of the intestinal barrier function using immunocytochemistry and image analysis as described in the online supplemental material and methods. This selection was based on: 1) established evidence showing that disruption of the apical junctional complex proteins like ZO-1 is a reliable marker of a disruption of intestinal barrier function[32 33] and 2) our finding that showed a robust and significant correlation between ZO-1 expression and urinary sucralose levels (online supplementary table S2).

Immunocytochemistry

Immunoperoxidase and immunofluorescence staining for the brain and gut samples were performed, as published previously[31] and explained in the online supplemental material and methods.

Microbiota analysis

Microbiota composition was interrogated in both human and mice using 16S ribosomal RNA sequencing as previously explained[9 34] and described in the online supplemental material and methods.

Statistical analyses

Experimental results are expressed as mean ±SEM. Differences between groups in the animal experiment were statistically analysed with a two-way analysis of variance (ANOVA) followed by a Tukey's multiple comparison test. Rotarod test results were analysed with a general linear model repeated measure ANOVA, with the within-subject factor time and the between-subject factor treatment (vehicle vs rotenone) and genotype (WT vs TLR4-KO). Pearson's correlations were applied to associate the different symptoms developed with rotenone exposure in mice. Results were considered statistically significant when p value was <0.05. Analyses were performed using SPSS V.22.0.

RESULTS

Part I: human study in subjects with PD and HC subjects

Subjects with PD showed intestinal barrier dysfunction

Bowel habit was assessed using a structured GI symptom severity index and Bristol stool score and none of the patients with PD had clinically significant constipation (online supplementary table S1). PD symptoms were assessed using the Unified Parkinson's Disease Rating Scale (UPDRS) and the modified Hoehn and Yahr scale (HYStage) (online supplementary table S1).[35 36] The current study confirmed intestinal hyperpermeability in subjects with PD (mean±SEM: 2.33%±0.30% sucralose excretion) compared with HC (0.97±0.28), as we reported previously.[8] Specifically, subjects with PD had significantly higher 24 hours urinary excretion of sucralose after ingestion of the sugar cocktail (n=6, unpaired two-tailed t-test: $t_{(10)}=3.36$, $p=0.01$; figure 1A). However, no group differences were observed in 5-hour urinary lactulose, mannitol or the lactulose/mannitol ratio (data not shown) suggesting that disruption of intestinal barrier function in patients with PD primarily involved the colon.

Intestinal barrier dysfunction permits the passage of bacteria and bacterial products such as LPS into the intestinal mucosa and the systemic circulation. LPS binds to the soluble acute-phase protein LBP presenting LPS to cell surface pattern receptors such as CD14 and TLR4, which are responsible for consequent innate immunity. Lower levels of LBP potentiate the cell's response to LPS by facilitating transfer of LPS molecules to its receptor CD14,[37] whereas higher levels of LBP inhibit cell responses to LPS by transferring the LPS to high-density lipoproteins[38] or by promoting internalisation of LPS without triggering inflammatory cell stimulation.[39] Similar to our previous report,[28] reduced levels of LBP were found in plasma samples from subjects with PD (15.73±3.75 µg/mL) compared with HC (33.47±6.20 µg/mL) subjects (n=5, unpaired two-tailed t-test: $t_{(8)}=2.45$, $p=0.04$; figure 1B).

The intestinal barrier is maintained by a series of junctional proteins including a major tight junction protein ZO-1. Immunofluorescence staining in HC displayed continuous expression of ZO-1 protein at the apical surface of the crypts (figure 1C-a,b). In contrast, ZO-1 immunofluorescence in PD cases was reduced in the colonic sigmoid mucosa (figure 1C-c,d). Average integrity scoring data per group showed significant disruption in the ZO-1 expression in subjects with PD (1.58±0.05) compared with HC subjects (2.32±0.18) for combined both apical junction of the crypts and epithelial lining (n=6, unpaired two-tailed t-test: $t_{(10)}=3.917$, $p=0.0029$; figure 1D). Taken together, these data demonstrate that patients with PD have disrupted colonic barrier integrity. Both the PD-associated reduced colonic ZO-1 expression and to a lesser extent increased urinary sucralose significantly correlated with enhanced colonic mRNA expression of inflammatory mediators and enhanced LBP plasma levels (ZO-1 scoring and LBP: $p<0.05$, $R=0.831$) (online supplementary table S2 and S3). Although these correlations does not equate to causation, these relationships allow us to infer potential causes.

Subjects with PD showed evidence of mucosal inflammation and immune activation

HC showed occasional TLR4 immunoreactivity in the lamina propria (figure 1E-a,b). This staining profile was enhanced in subjects with PD (figure 1E-c,d). Analyses of TLR4+ cells in the lamina propria supported the qualitative observations. In this regard, HC displayed (41.30±9.76) cells; an estimate significantly lower that PD cases (127.9±30.47) (n=6; unpaired two-tailed t-test: $t_{(10)}=2.71$, $p=0.02$, figure 1F). For further evaluation, immunofluorescence staining was performed. Confocal microscope showed restricted TLR4 immunoreactivity to the apical surface of the crypt in samples from HC with minimal expression in the lamina propria. In comparison to HC subjects, biopsies from subjects with PD showed TLR4 immunoreactivity at the apical surface and the basolateral surface of the crypts but importantly TLR4 immunoreactivity was also observed in the lamina propria of colonic tissue. These data demonstrate that PD is associated with an increase in TLR4+ cells in the intestinal mucosa.

Occasional CD3+ T cells were observed in the lamina propria of HC samples (figure 1G-a,b). These cells were in close proximity to the basolateral surface of the crypts. In contrast, subjects

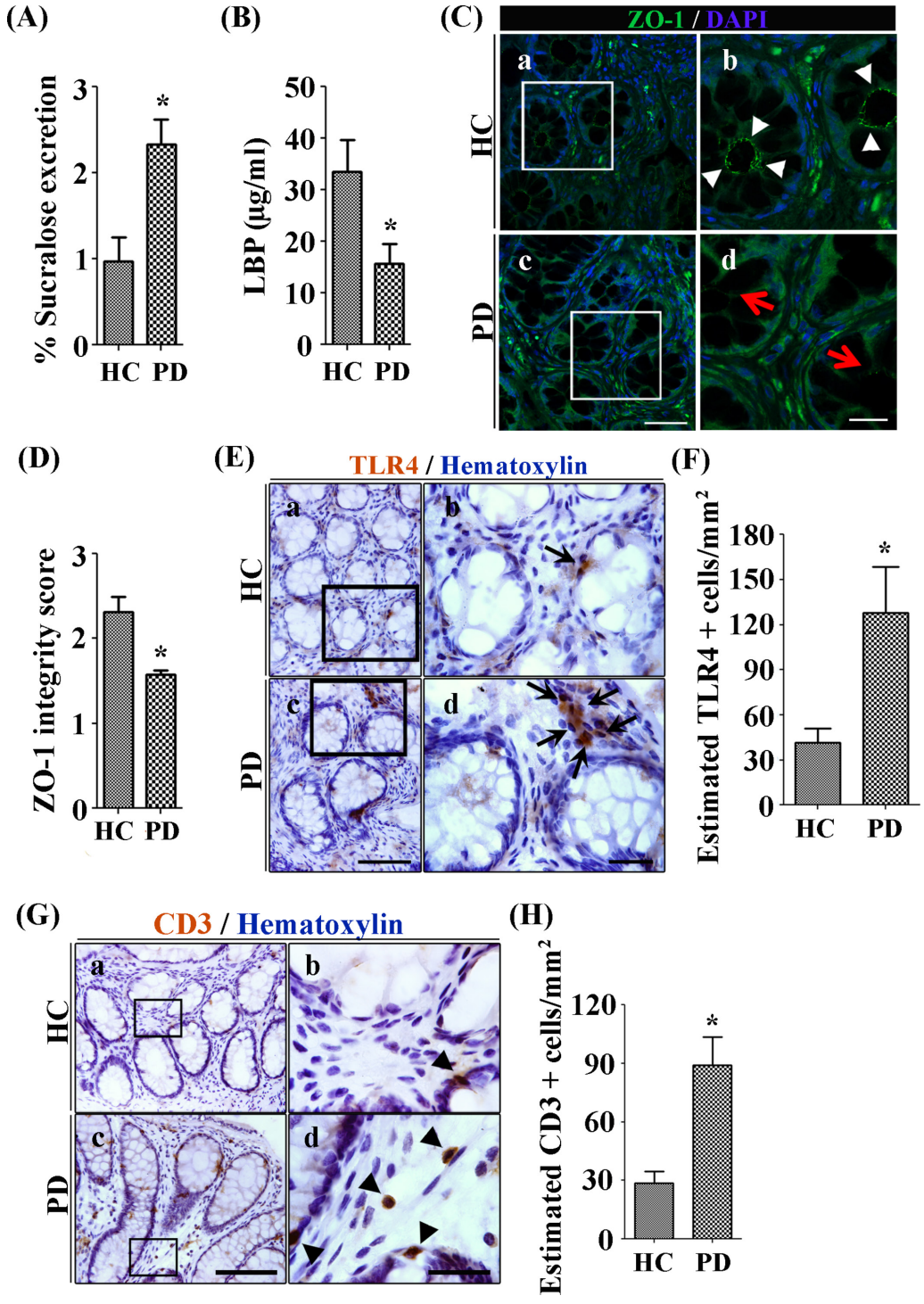

Figure 1 Patients with Parkinson's disease (PD) show increased colonic permeability and associated colonic inflammatory as well as immune markers in their biopsies compared with healthy controls (HC). (A) Per cent excretion of sucralose in the urine samples as an intestinal permeability marker. (B) Levels of LPS-binding protein (LBP) as a marker for systemic endotoxin in plasma samples. (C) Photomicrographs of immunofluorescence staining of tight junction protein zonula occludens 1 (ZO-1) in HC (a, b) and PD (c, d) colonic mucosa. (D) Integrity scoring for ZO-1 tight junction protein expression in colonic samples. (E) Photomicrographs of stained toll-like receptor 4 (TLR4)+ cells in lamina propria of the HC (a, b) and PD mucosa (c, d). (G) Photomicrographs of stained CD3+ T cells in colonic mucosa of HC (a, b) and PD (c, d). (H) Assessment of CD3+ cells in lamina propria of colonic samples. Scale bars: C(c)=50 µm and C(d)=20 µm, E(c)=75 µm and E(d)=25 µm, G(c)=40 µm and G(d)=25 µm. *P<0.05, **p<0.001, ***p<0.0001. Data represent mean±SEM.

with PD showed higher CD3+ T-cell numbers in the lamina propria as opposed to being in close proximity to the basolateral surface (figure 1G-c,d). Analyses showed a significantly greater number of CD3+ T cells in the lamina propria of patients with PD (89.02±14.43) compared with HC (28.63±5.89) (n=6; unpaired two-tailed t-test: $t_{(10)}=3.87$, p<0.001; figure 1H). These data demonstrate that CD3+ cells have penetrated the intestinal mucosa in subjects with PD.

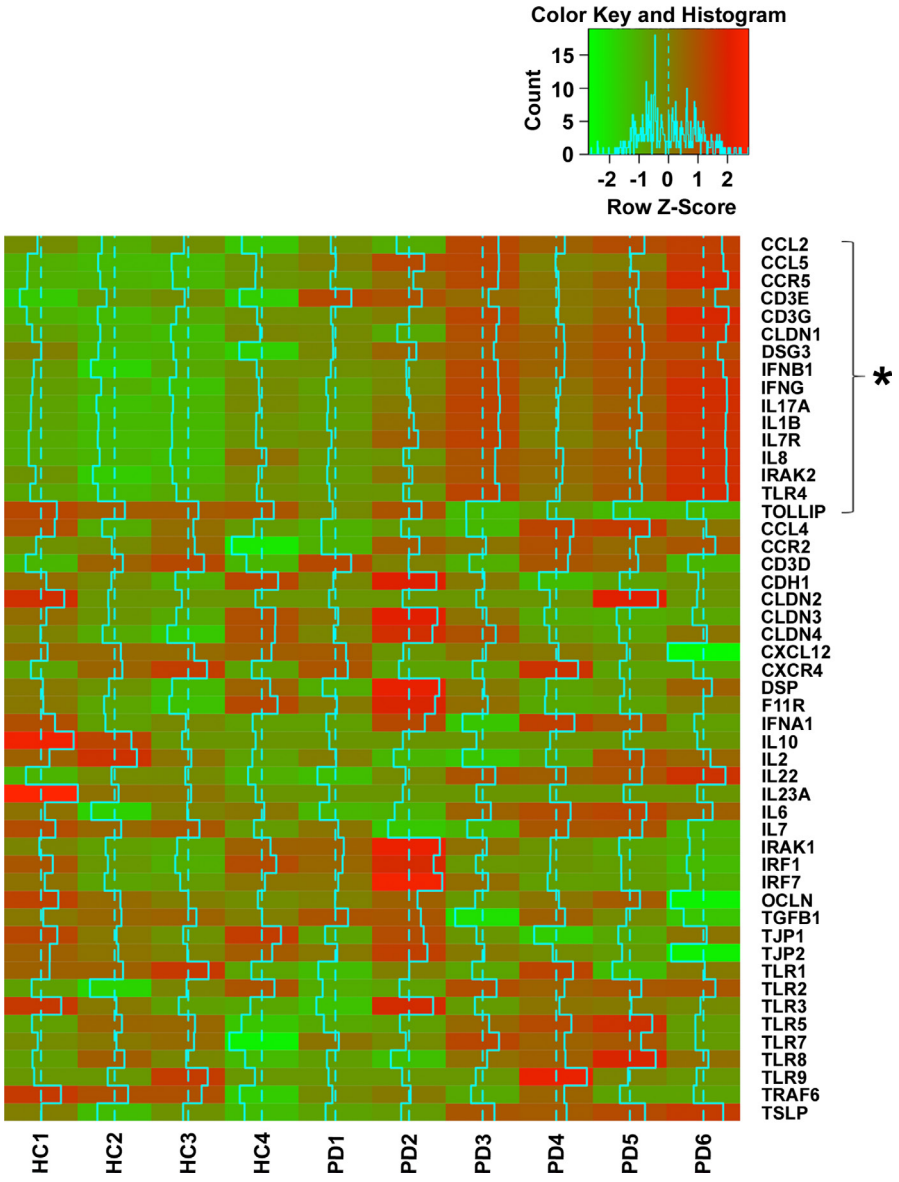

Figure 2 Higher pro-inflammatory milieu was observed in the colonic biopsies of subjects with Parkinson's disease (PD) compared with healthy control (HC) subjects. Genes specific for microbiota-induced intestinal inflammation and gut dysfunction were evaluated from HC subjects (HC1, HC2, HC3 and HC4) and subjects with PD (PD1, PD2, PD3, PD4, PD5, PD6). *P<0.03 denotes significantly different gene in PD compared with HC. Green colour indicates lower expression and red colour indicates higher expression of gene.

To further characterise the immune pathways and inflammation in PD mucosa, a microarray analysis was performed on sigmoid mucosal samples including 50 genes relevant to microbial translocation and inflammatory pathways (figure 2). Out of 50 genes, 15 were significantly upregulated and 1 gene was significantly downregulated in biopsies obtained from subjects with PD compared with HC subjects. In agreement with the histological findings, there was significantly higher TLR4 mRNA expression in PD biopsies compared with those from HC. Downstream signalling molecules associated with TLR4 activation were altered in a way that was consistent with increased TLR4 signalling. Increased IRAK2 expression was observed while levels of the inhibitory molecule TOLLIP was significantly lower in colonic biopsy tissue from subjects with PD compared with HC subjects (figure 2). Cytokines (interleukin (IL)-1β, interferon (IFN)-γ, CCL5 (RANTES)) and chemokines (CCL2, CCL5, CCR5) were elevated in PD sigmoid mucosa compared with HC (figure 2). In addition, tissue from subjects with PD had significantly more mRNA expression of CD3+ T-cell markers (CD3G, CD3E) and T helper (Th)1/Th17 inflammatory cytokines (IFN-γ, IL-1β, IFN-β, IL-17A, IL-8) and IL-7R compared with tissue from HC subjects. These data are consistent with increased activation of TLR4 and/or CD3+ immune activation. There were no significant changes in the mRNA levels of other TLRs.

Microbiota composition of subjects with PD showed decreased short chain fatty acids producers

Microbiota composition in these 6 patients with PD has already been reported as part of our larger cohort of 38 patients with PD[9] and changes observed in these 6 patients were similar to our prior report. At the taxonomic level of genus, putative 'anti-inflammatory' SCFA-butyrate producing bacteria were less abundant in PD versus HC mucosa and faecal samples (online supplementary table S4). Compared with HC subjects, the genus *Dorea*

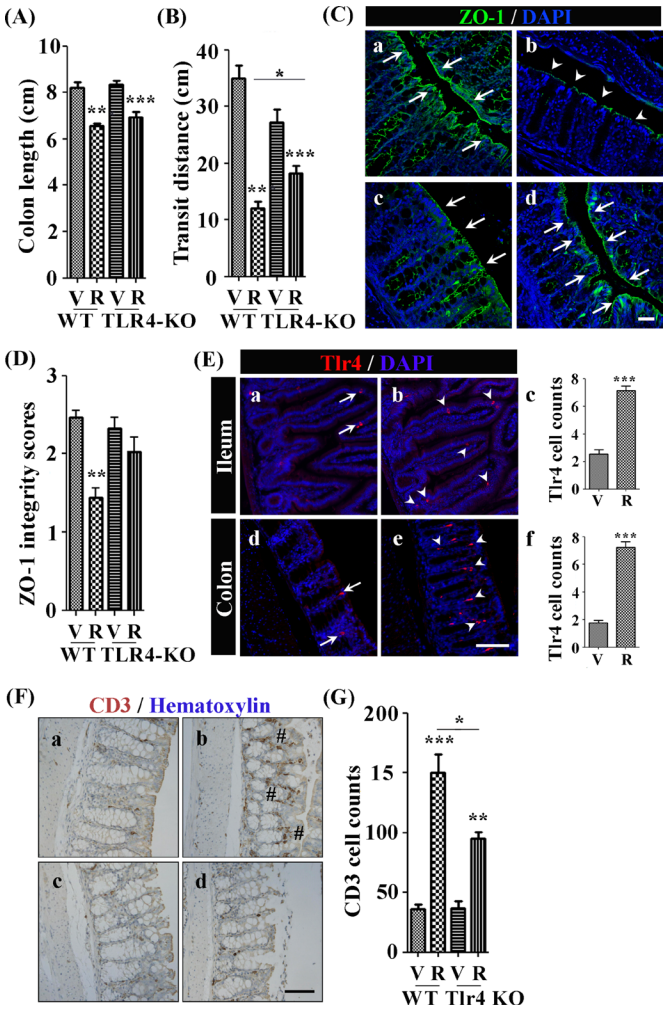

Figure 3 Rotenone Parkinson's disease (PD) model recapitulates GI physiology as observed in human patients with PD and toll-like receptor 4 (TLR4)-knockout (KO) partially protects against them. (A) Colon length. (B) Intestinal transit distance. (C) Photomicrographs of immunofluorescence staining for zonula occludens 1 (ZO-1). (D) ZO-1 integrity scores. (E) Photomicrographs of TLR4 immunofluorescence staining. Graphs represent TLR4+ cell counts in (c) ileum and (f) colon samples. (F) Photomicrographs of CD3 stained cells in colonic samples. Black number sign (#) in panel (b) represent increased CD3+ T cells infiltration into lamina propria. (G) Quantitative analyses of cell counts for CD3+ T cells in lamina propria. Scale bars C(d), E(e), F(d)=100 µm. ***P<0.001, **P< 0.01, *P< 0.05. Data represent as mean+SEM.

Log2FC relative abundance decreased greatly in PD mucosa; genera *Roseburia* and *Anaerostipes* Log2FC relative abundances decreased the most in PD faecal samples (online supplementary table S4).

Part II: rotenone-induced PD mouse model

TLR4-KO mice are partially protected from rotenone-induced effects on the intestine

The rotenone model recapitulated several aspects of intestinal dysfunction associated with PD. Rotenone-treated mice showed a reduction in colon length compared with vehicle-treated ($p<0.0001$; figure 3A) as well as a delayed intestinal transit (ie, reduced distance travelled by the Evans Blue dye in the intestinal tract) ($F_{(1,26)}=81.53$, $p<0.0001$; figure 3B). WT-vehicle-treated mice had an intact tight junction barrier with a continuous lattice pattern around the epithelial lining in colon. In contrast, WT-rotenone mice showed reduced/disrupted levels of ZO-1 expression ($p<0.01$) (figure 3C, D) comparable to observations in human subjects with PD (figure 1C).

Similar to human PD biopsy tissue, rotenone-treated mice demonstrated increased numbers of TLR4+ cells and CD3+ cells in the intestinal mucosa relative to vehicle-treated mice. Rotenone-treated mice had a greater number of TLR4+ cells in the mucosa of colon tissue while control mice showed occasional TLR4 expression in close proximity to basolateral crypts. Specifically, rotenone-treated mice had evidence of immune activation with a higher number of TLR4+ cells in the ileum and the colon compared vehicle-treated mice (figure 3E, F) ($p<0.0001$). Stereological analyses showed increased number of CD3+ T cells in the colon of WT rotenone-treated mice compared with vehicle-treated mice (figure 3G); again in accordance with what we saw in PD human study (figure 3G).

To establish whether TL4 was critical for this effect, we examined the effects of rotenone in TLR4-KO mice. TLR4-KO did not impact rotenone-induced decrease in colon length (figure 3A); however, the TLR4-KO mice were partially protected from rotenone-induced deficits in intestinal transit time ($p<0.05$) (figure 3B). Finally, while rotenone significantly decreased ZO-1 integrity in WT mice, the TLR4-KO mice were protected from disruptive effects of rotenone on intestinal barrier integrity (figure 3C, D).

Rotenone-induced increase in CD3+ T cells in the mucosa of WT mice was mitigated in TLR4-KO mice ($F_{(1,36)}=91.98$, $p<0.0001$, figure 3G, H). There was a significant main effect of genotype ($F_{(1,36)}=8.97$, $p<0.01$) as well as an interaction effect between treatment (rotenone vs control) and genotype ($F_{(1,36)}=9.30$, $p<0.01$).

Our next step was to determine if these changes in immune markers are accompanied by biological changes. Thus, we assessed GFAP as a marker of enteric glial activity and α-syn accumulation in the myenteric plexus. While WT-rotenone group showed an increased number of GFAP+ enteric glial cells in myenteric plexuses compared with WT-vehicle the TLR4-KO, rotenone-treated mice had mitigated expression of GFAP+ enteric glial cells (figure 4A). Analyses showed increased GFAP staining in the myenteric plexuses of WT-rotenone mice while TLR4-KO mice were unaffected ($F_{(1,36)}=9.25$, $p<0.01$; figure 4B). There was a significant main effect of genotype ($F_{(1,36)}=7.86$, $p<0.01$) and an interaction between genotype and treatment ($F_{(1,36)}=9.15$, $p<0.01$). Post hoc analysis showed that GFAP intensity in myenteric plexuses of TLR4-KO-rotenone group was similar to TLR4-KO-vehicle and WT-vehicle but it was significantly lower than the WT-rotenone group ($p<0.01$). Analyses showed higher α-syn positive structures in the myenteric plexuses (figure 4C) of WT-rotenone compared with other groups. There was no difference in α-syn immunoreactivity between WT-vehicle, TLR4-KO-vehicle and TLR4-KO-rotenone (figure 4C). Optical density analyses for α-syn intensity (figure 4D) in the myenteric plexuses showed an increased α-syn expression in WT-rotenone ($F_{(1,36)}=34.19$, $p<0.0001$). There was an effect of the genotype on α-syn expression in the colon ($F_{(1,36)}=28.68$, $p<0.0001$) and an interaction between treatment and genotype ($F_{(1,36)}=24.82$, $p<0.0001$). Post hoc analysis revealed lower levels of α-syn in TLR4-KO-rotenone group compared with WT-rotenone ($p<0.0001$).

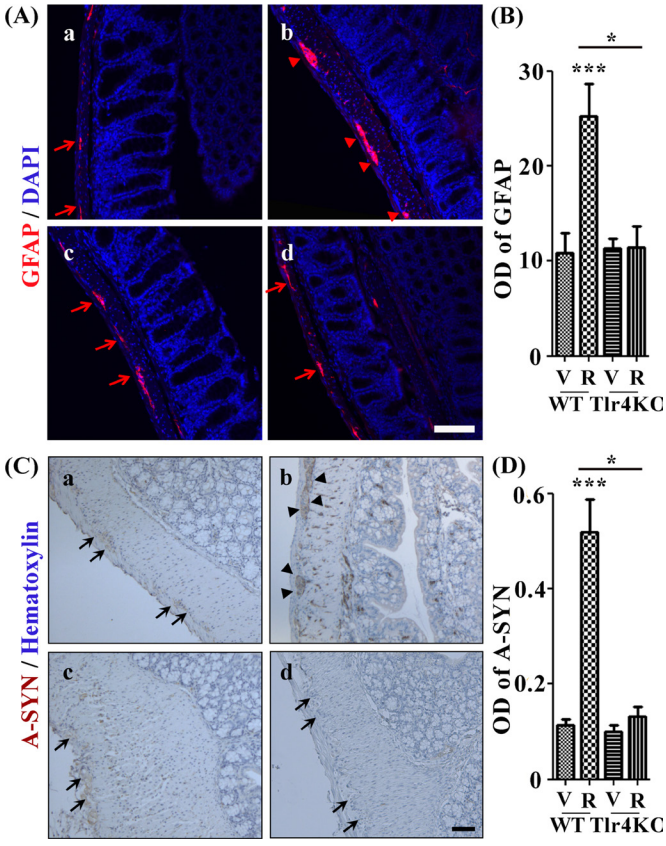

Figure 4 Toll-like receptor 4 (TLR4)-knockout (KO) mice were partially protect against rotenone-induced enteric glial inflammation and α-syn expression in the colon. Photomicrographs represent histology for (A) GFAP and (C) α-syn markers in colon. (B) Quantitative analyses of optical density (OD) data for GFAP in myenteric plexuses and (D) OD data for α-syn expression in myenteric plexuses. Scale bars A(d), C(d)=100 µm. Scale bar in panel represents 100 µm. *P<0.05, ***p<0.0001. Data represented as mean+SEM.

TLR4-KO mice are partially protected from rotenone-induced effects in the brain

Microglia are morphologically and functionally dynamic CNS cells, on activation microglia transform from thin cell bodies with highly ramified extensions into amoeboid cells with fewer branches[40] with these morphological changes indicative of a transition to pro-inflammatory/phagocytic microglia. This analysis focused on the SN, a region highly relevant for PD. Compared with vehicle-treated WT mice, microglia in WT-rotenone animals displayed a decreased number of branches (p<0.001, figure 5A), decreased number of branch end points (p<0.01, figure 5B), decreased branch length (p<0.05, figure 5C) and increased ratio of cell body size/total cell size (p<0.01, figure 5D). A comparison between WT and TLR4-KO rotenone-treated mice revealed that TLR4-KO mice had significantly more branches (p<0.05), branch length and a decrease in the ratio of cell body size/total cell size compared with WT-rotenone mice (p<0.01). Rotenone treatment in WT or TLR4-KO mice resulted in a similar reduction of number of branches end points.

Tyrosine hydroxylase (TH) staining was performed to assess the number of dopaminergic neurons in PD relevant brain areas. Analyses showed significantly lower number of TH+ cells in the SN after rotenone treatment in WT group compared with vehicle (figure 5F). In WT mice, rotenone significantly reduced the number of TH+ cells in the SN; however, rotenone treatment in TLR4-KO mice impacted the number of TH+ cells to a lesser extent (figure 5F). Cell count analyses showed significantly decreased number of TH+ cells in the SN in WT-rotenone group compared with others ($F_{(1,36)}$=35.89, p<0.0001) (figure 5G). There was a significant interaction between treatment (rotenone vs vehicle) and genotype (WT vs KO) ($F_{(1,36)}$=6.48, p<0.05). Post hoc analysis showed that the WT-rotenone group had significantly lower number of TH+ cells compared with TLR4-KO-rotenone mice (p<0.05) (figure 5G).

A rotarod test was used to assess motor function and data are represented as latency to fall in seconds (figure 5H). There was an overall effect of treatments (rotenone vs vehicle) ($F_{(1,32)}$=60.11, p<0.0001) and of genotype ($F_{(1,32)}$=9.60, p<0.01) on rotarod performance. Repeated measures showed an effect of time ($F_{(3,96)}$=22.49, p<0.0001). WT-rotenone group showed greater motor dysfunction over time compared with WT-vehicle (interaction effect treatment×time $F_{(3,96)}$=1.33, p<0.0001). WT-rotenone mice showed a decrease in rotarod performance starting on day 21 compared with the WT-vehicle ($F_{(1,32)}$=6.20, p<0.05 on day 21 and $F_{(1,34)}$=72.14, p<0.0001 on day 28). On day 28, there was a significant effect of the genotype ($F_{(1,34)}$=8.05, p<0.001) on rotarod performance. Post hoc analysis showed that TLR4-KO-rotenone mice performed significantly better on the rotarod compared with WT-rotenone (p<0.05) (figure 5H).

Evidence to support the gut-immune-brain axis involvement in rotenone-induced PD mice

In an effort to understand how multiple variables are similar or dissimilar from each other, correlation analysis was performed. While correlation does not equate to causation, these relationships allow us to infer potential relationships. ZO-1 integrity score inversely associated with the number of CD3+ T cells in colon (r=−0.64, p<0.0001; figure 6A). The number of T cells in colon positively correlated with α-syn in the colon (r=0.59, p<0.0001; figure 6B). α-Syn in the colon positively correlated with a marker of microglial activation in the SN (ie, the ratio of microglial cell body size/total cell size) (r=0.76, p<0.0001; figure 6C). Likewise, presence of phagocytic-like microglial phenotype in the SN (increased ratio cell body size/total cell size) inversely correlated with the number of dopaminergic cells (TH+ cells) in the SN (r=−0.63, p<0.01; figure 6D). Finally, the number of dopaminergic cells in the SN positively correlated with motor function (latency to fall in the rotarod) (r=0.72, p<0.0001; figure 6E).

TLR4-KO mice exerts aforementioned beneficial effects despite rotenone-induced altered mucosal and luminal microbiome profile

We assessed both caecal mucosa and caecal luminal microbiota in WT and TLR4-KO (with or without rotenone treatment) mice. As previously reported,[34] we confirmed that rotenone treatment impacted both caecal mucosal-associated and luminal microbiota. In addition, we now show that TLR4-KO mice have an altered microbiota profile (a genotype effect) irrespective of rotenone treatment.

Alpha diversity, richness showed a significant rotenone treatment effect, only in the caecum mucosa (two-way ANOVA: $F_{(1,36)}$=12.97, p=0.0009). There was no significant effects of genotype or an interaction between rotenone and genotype (p>0.05). Rotenone resulted in significantly higher richness in the WT-rotenone compared with WT-vehicle mice (p<0.001) (figure 7A). The other alpha diversity indices (Simpson index, Shannon index and evenness) showed no significant changes

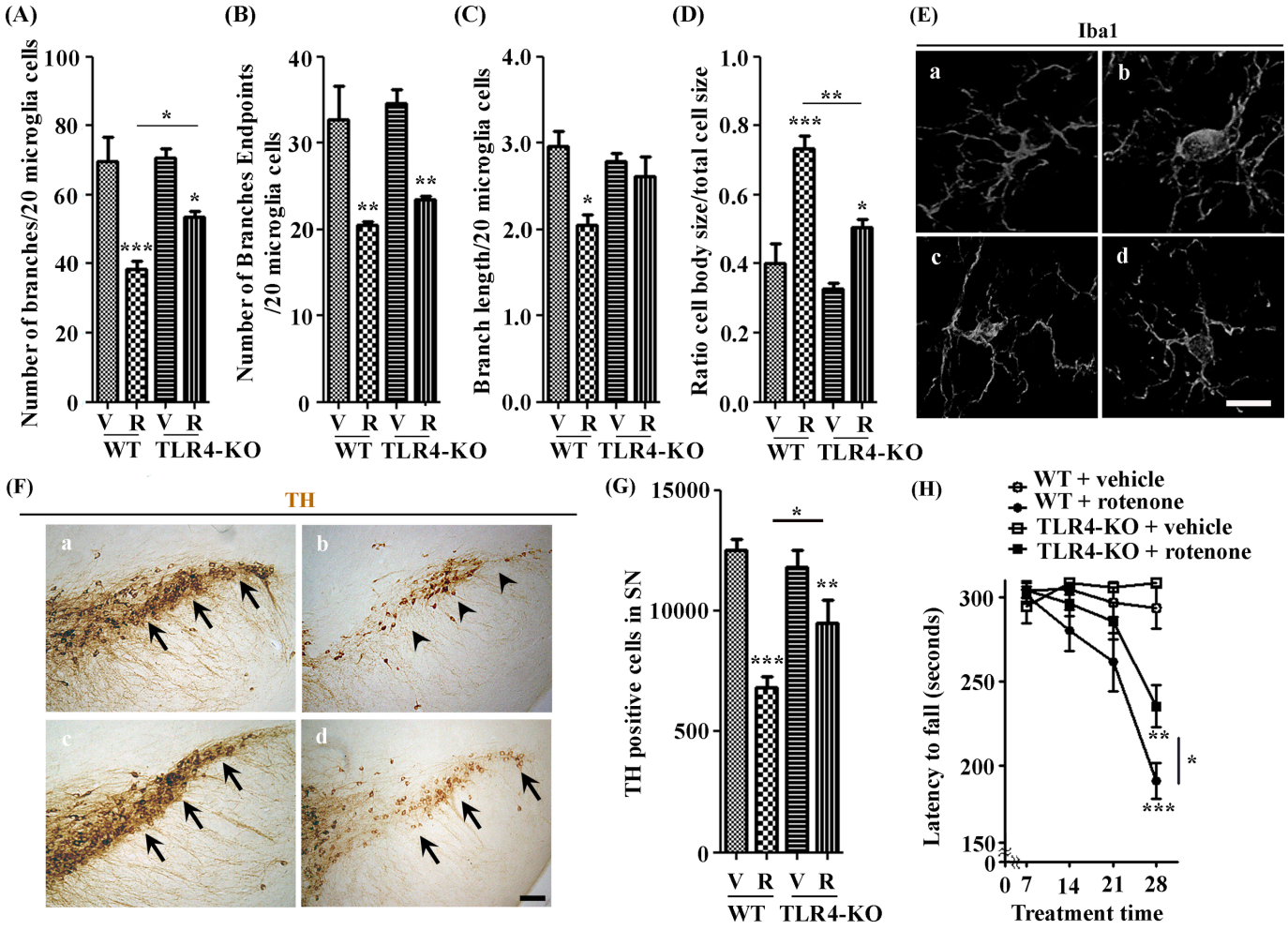

Figure 5 Toll-like receptor (TLR4)-knockout (KO)-rotenone mice showed less pro-inflammatory microglia, less dopaminergic cell loss and less behaviour deficits compared with wild-type (WT)-rotenone. (A–D) Average number of branches, branches end points, branch length and the ratio cell body size/total cell size of microglia in the substantia (SN). (E) Photomicrographs of microglial cells for each condition. TLR4-KO mice showed microglia with less pro-inflammatory phenotype in the SN compared with WT-rotenone mice. (F) Photomicrographs of tyrosine hydroxylase (TH) stained dopaminergic cells. (G) Cell counts for TH stained dopaminergic cells into SN. WT-rotenone showed profound loss of TH cells while TLR4-KO-rotenone showed a mitigated TH+ cell loss in the SN. (**H**) Rotarod data to assess motor function associated behaviour deficits. TLR4-KO-rotenone group showed reduced rotenone-induced motor-dysfunction compared with WT-rotenone. Scale bars: E(d)=10 µm, F(d)=200 µm. *P<0.05, **p<0.001, ***p<0.0001. Data represented as mean+SEM.

with either rotenone or genotype in both samples sites (data not shown).

On examining the beta diversity, at the taxonomic level of genus, the overall microbial community structures were globally significantly different (ANOSIM mucosa: Global R=0.635; p=0.001; ANOSIM luminal content: Global R=0.572; p=0.001) (figure 7B) in both the caecal mucosa and luminal content. Specified significant differences between two mouse group comparisons (eg, WT-vehicle vs WT-rotenone; WT-vehicle vs TLR4-KO-vehicle (genotype)) are depicted in the online supplementary table S5.

Firmicutes-to-bacteroidetes (F/B) ratio is a reliable marker of global change in microbiota community between different experimental groups and it is an established predictors of the host SCFA level[41] (figure 7C). In caecal mucosa, the F/B ratio showed a significant effect of rotenone treatment (two-way ANOVA: $F_{(1,35)}$=5.135, p=0.0297), geneotype effect (two-way ANOVA: $F_{(1,35)}$=9.391, p=0.0042) and interaction between rotenone and genotype effect (two-way ANOVA: $F_{(1,35)}$=6.149, p=0.0181). Post hoc analysis showed a significantly lower F/B ratio in WT-rotenone compared with WT-vehicle (p<0.01). Also, TLR4-KO-vehicle mice showed a significantly lower F/B ratio compared with WT-vehicle (p<0.001), but TLR4-KO-rotenone mice showed no significant changes compared with TLR4-KO-vehicle (figure 7C). Compared with the caecal mucosa, the F/B ratio in the luminal content samples only showed a significant effect of interaction between rotenone and genotype effect (two-way ANOVA: $F_{(1,34)}$=5.243, p=0.0284). Post hoc analysis showed a significantly lower F/B ratio in TLR4-KO-vehicle compared with WT-vehicle (p<0.05) (figure 7C). Overall, these data suggest that irrespective of vehicle/rotenone treatment, the TLR4-KO mice showed significantly lower F/B ratio compared with WT-vehicle and rotenone treatment resulted in lower F/B ratio in only WT mice.

Individual taxa differences, at the taxonomic level of genus were evaluated in all groups (figure 7D, E). Overall, the caecum mucosa taxa relative abundance differences were greater than the luminal content taxa (figures 7D, E, 8A and 9A). To further characterise the taxa differences, we performed two mice model comparisons and the results are depicted in figures 8B-E and and 9B-E.

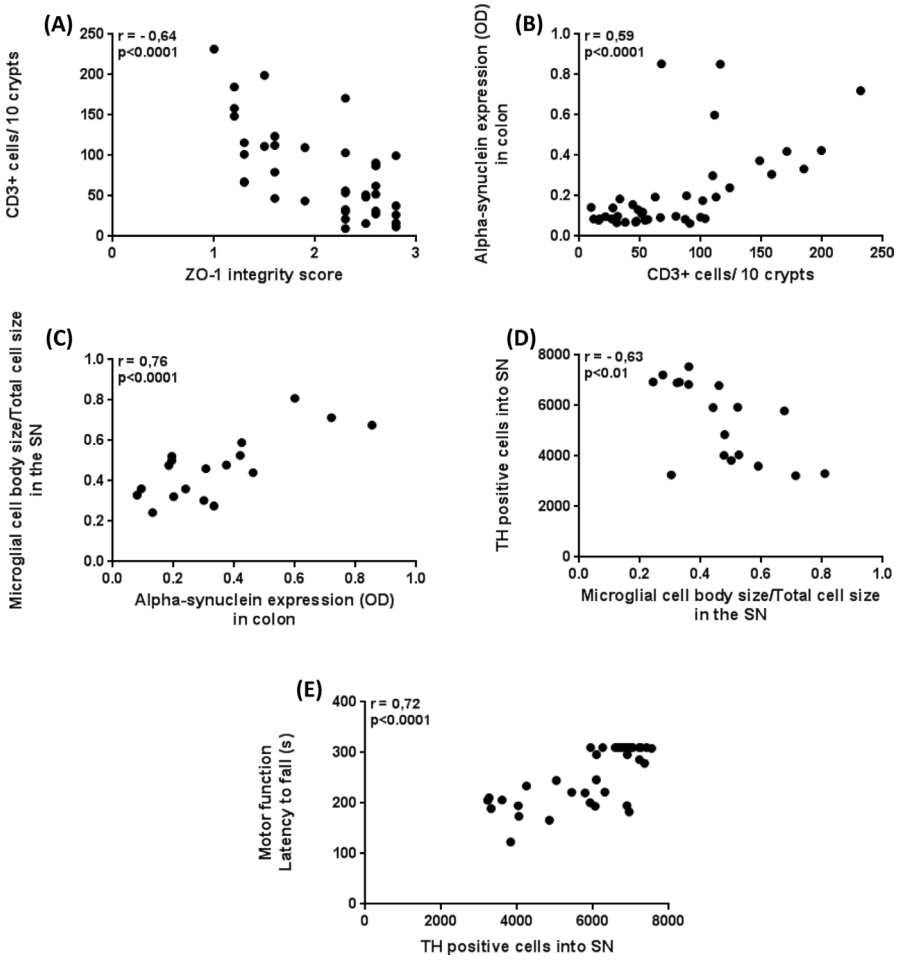

Figure 6 Correlations support the gut-immune-brain axis involvement in rotenone-induced Parkinson's disease (PD)-like in mice. (A) Zonula occludens 1 (ZO-1) integrity score, decreased with rotenone treatment, was inversely associated with the number of T cells in colon. (B) The number of T cells in colon, significantly increased with rotenone, was positively associated with alpha-synuclein (α-syn) expression in colon. (C) α-Syn expression in colon was positively correlated with the ratio microglial cell body size/total cell size in the substantia (SN). Rotenone exposure changed microglial phenotype into a more pro-inflammatory state (increased ratio cell body size/total cell size) in the SN. (D) This state inversely correlated with the number TH+ cells in the SN. (E) The number of TH+ cells in the SN, decreased after rotenone exposure, was positively associated with motor function (latency to fall in the rotarod).

Overall, the caecal mucosa samples showed that rotenone treatment in WT mice resulted in significantly increased (FDR-p<0.05) relative abundances of bacterial genera unclassified Rikenellaceae, unclassified *S24-7*, unclassified Clostridiales and *Allobaculum* compared with WT-vehicle mice (figure 8B); rotenone treatment in TLR4-KO mice resulted in an increase (FDR-p<0.05) in the relative abundances of bacterial genera unclassified Lachnospiraceae, unclassified Clostridiales and *Lactobacillus* compared with TLR4-KO-vehicle mice (figure 8C). Importantly, rotenone treatment in both WT and TLR4-KO mice showed a significant decrease (FDR-p<0.05) in the relative abundance of the putative beneficial genus *Bifidobacterium*, in caecal mucosa samples. Similar, but less marked relative abundance taxa changes were noted in the caecum luminal content (figure 9B and C).

When examining the caecal mucosa for the TLR4-KO genotype effect, TLR4-KO-vehicle mice showed significant increase (FDR-p<0.05) in the relative abundances of putative 'pro-inflammatory' bacterial genera unclassified Rikenellaceae, unclassified *S24-7* and *Bacteroides*; decrease (FDR-p<0.05) in the relative abundances of genera of putative 'beneficial' *Bifidobacterium* and *Lactobacillus*, compared with WT-vehicle mice (figure 8D). In addition, TLR4-KO-rotenone mice only showed a significant decrease (FDR-p<0.05) in the relative abundance of the genus *Lactobacillus* compared with WT-rotenone (figure 8E). Similar, but less marked relative abundance individual taxa changes were noted in the caecum luminal content. Overall, these data suggest that TLR4-KO mice showed altered microbiota profiles and rotenone treatment resulted in similar microbiota profiles irrespective of the genotype.

DISCUSSION

Several studies have demonstrated that neuroinflammation and oxidative stress are involved in α-syn misfolding and aggregation.[42–46] We[9] and others[12 13 18] have proposed that the trigger for this neuroinflammation and immune activation in the brain is the gut microbiota. There is a plethora of literature showing that manipulation of the intestinal microbiota influences brain function and inflammation.[47–49] More specifically, we[9] and others[12 13 15 17 50–53] have shown a pro-inflammatory dysbiotic microbiota community in patients with PD. Accordingly, we hypothesised that dysbiotic microbiota will trigger mucosal immune activation in the colon through TLR4 signalling pathway, leading to neuroinflammation and neurodegeneration in PD.

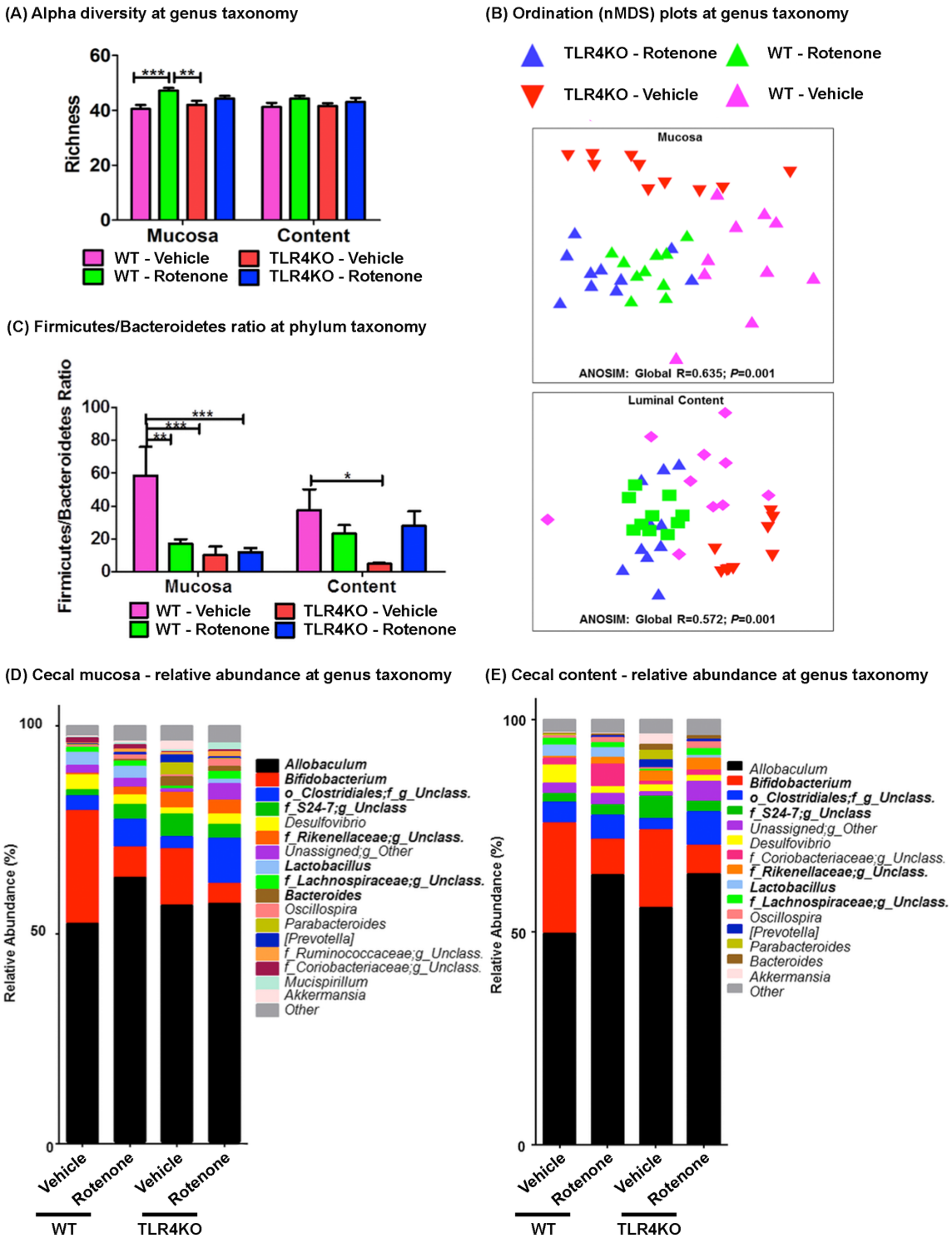

Figure 7 Microbiome analysis assessing mice wild type (WT) or toll-like receptor 4 (TLR4)-knockout (KO) (with or without rotenone treatment). (A) Caecal sample sites were examined for alpha diversity's richness between all four mouse groups, at the taxonomic level of genus. Data expressed as mean+SEM and analysed with two-way analysis of variance (ANOVA): within the caecum mucosa, richness showed a significant rotenone treatment effect ($F_{(1,36)}$=12.97, p=0.0009). Bonferroni post hoc test: **p=0.01, ***p=0.001. (B) Ordination plots (nMDS plots) of microbial community structure at the taxonomic level of genus, using analysis of similarity ANOSIM (Global R and P values shown), comparing WT-vehicle (pink triangles), WT-rotenone (green triangles), TLR4-KO-vehicle (red triangles) and TLR4-KO-rotenone (blue triangle) treated mice caecum mucosa and luminal content samples. (C) Firmicutes-to-bacteriodetes (F/B) ratio comparisons between mice caecal sample sites, at the taxonomic level of phylum. Data expressed as mean+SEM and analysed with two-way ANOVA: F/B ratio in the caecal mucosa showed a significant rotenone treatment effect ($F_{(1,35)}$=5.135, p=0.0297), geneotype effect ($F_{(1,35)}$=9.391, p=0.0042) and interaction between rotenone and genotype effect ($F_{(1,35)}$=6.149, p=0.0181). The F/B ratio in the luminal content showed a significant effect of interaction between rotenone and genotype effect ($F_{(1,34)}$=5.243, p=0.0284). Bonferroni post hoc test: *p=0.05, **p=0.01, ***p=0.001. (D, E) Caecal mucosa and luminal content stacked column plots depicting the relative abundances of individual bacterial genera (<1%); significant (FDR-p) genus taxa are bolded.

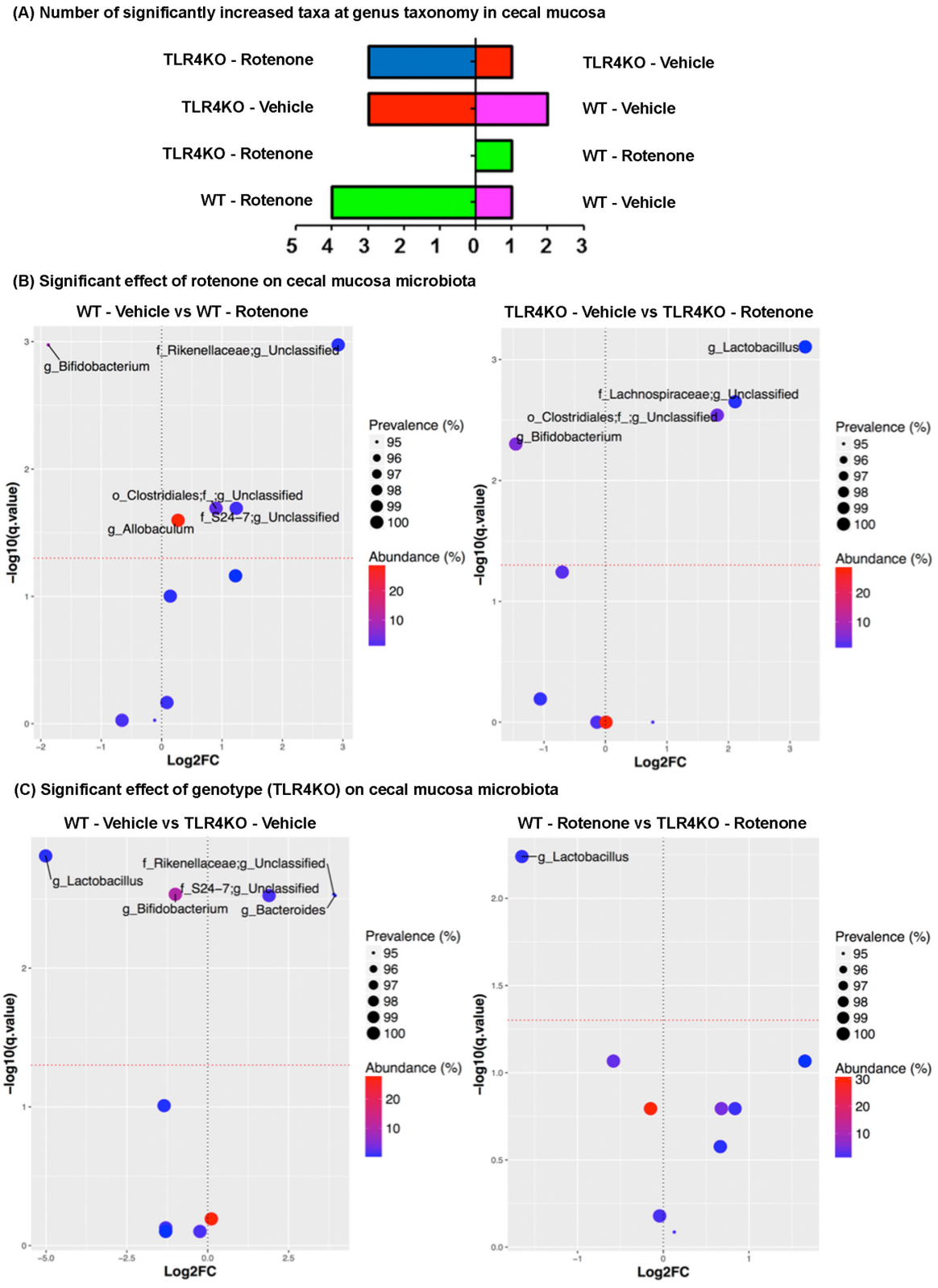

Figure 8 Caecum mucosa differential abundances of genus taxonomic level operational taxonomic units (OTU). (A) The number of significantly increased relative abundant genus taxa (FDR-p), per mouse caecal mucosa group. Volcano plot of estimated log2 fold change (FC) differences in genus (OTU) abundance between: effect of rotenone, (B) wild-type (WT)-vehicle vs WT-rotenoneand toll-like receptor 4 (TLR4)-knockout (KO)-vehicle vs TLR4-KO-rotenone; effect of TLR4-KO genotype, (C) WT-vehicle vs TLR4-KO-vehicleand WT-rotenone vs TLR4-KO rotenone, with corresponding Benjamini-Hochberg adjusted FDR-p values (q), derived from Kruskal-Wallis test in R programing language. The red dotted line indicates the 5% false discovery threshold. Prevalence indicates percentage of mice groups in which a given genus OTU is present. Abundance indicates mean relative abundance (%) of a given genus OTU. Name of genus OTUs differentially abundant at FDR≤5% are given at the lowest classified rank in Greengenes (Greengenes ID). The parameter log2FC was calculated for each mouse group according to the formula log2FC=log2(mean intervention/mean control). o, order; f, family; g, genus.

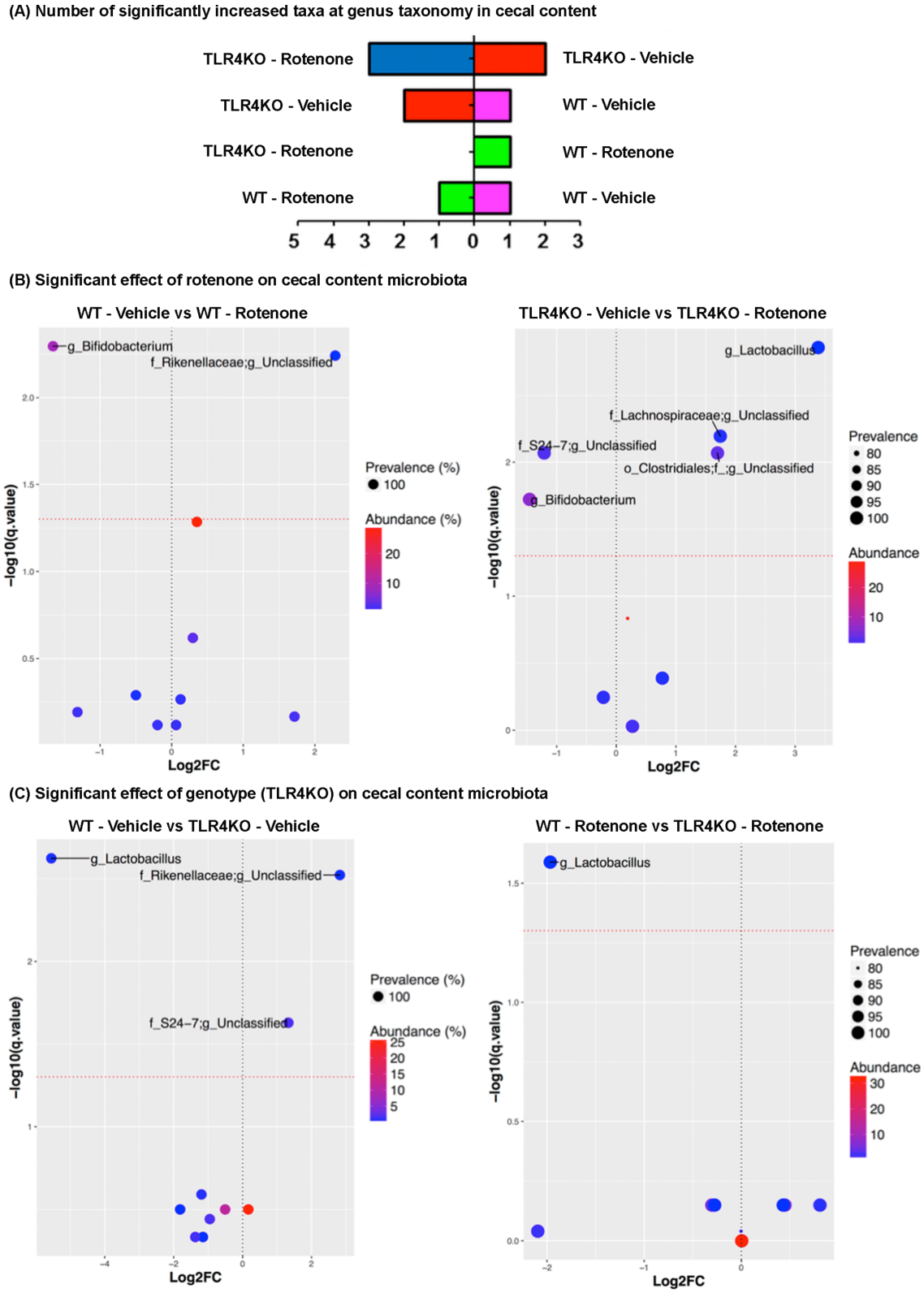

Figure 9 Caecum luminal content differential abundances of genus taxonomic level operational taxonomic units (OTU). (A) The number of significantly increased relative abundant genus taxa (FDR-p), per mouse caecal luminal content group. Volcano plot of estimated log2 fold change (FC) differences in genus (OTU) abundance between: effect of rotenone, (B) wild-type (WT)-vehicle vs WT-rotenone and toll-like receptor 4 (TLR4)-knockout (KO)-vehicle vs TLR4-KO-rotenone; effect of TLR4-KO genotype (C)WT-vehicle vs TLR4-KO-vehicle, (E) WT-rotenone vs TLR4-KO rotenone, with corresponding Benjamini-Hochberg adjusted FDR-p values (q), derived from Kruskal-Wallis test in R programing language. The red dotted line indicates the 5% false discovery threshold. Prevalence indicates percentage of mice groups in which a given genus OTU is present. Abundance indicates mean relative abundance (%) of a given genus OTU. Name of genus OTUs differentially abundant at FDR≤5% are given at the lowest classified rank in Greengenes (Greengenes ID). The parameter log2FC was calculated for each mouse group according to the formula log2FC=log2(mean intervention/mean control). o, order; f, family; g, genus.

This hypothesis was based on published findings that patients with PD had: (1) dysbiotic microbiota community hallmarked by increased abundance of endotoxin-producing bacteria,[9] (2) leakiness to endotoxin (LPS) and evidence of systemic endotoxin leak as serum LBP was increased in patients with PD.[8 28] To test our hypothesis, we first assessed TLR4 pathway in the colonic mucosa of patients with PD. We elected to study colonic (sigmoid tissue) because: (1) patients with PD have primarily colonic intestinal hyperpermeability and not small bowel hyperpermeability with LPS translocation in their colonic mucosal samples[8] and (2) SCFA levels, fermentation products of the colonic bacteria, were significantly lower in the stool of patients with PD than healthy.[13] As we predicted, we found a pro-inflammatory state in the colon of patients with PD evident by increased presence of CD3+ T cells, TLR4+ cells, increased pro-inflammatory cytokines and chemokines and decreased abundance of SCFA-producing colonic bacteria in colon tissues of subjects with PD. Increased T-cell trafficking into the colonic mucosa is a feature associated with PD. A recent study reported increased T-cell trafficking into colonic mucosa of constipated patients with PD.[21] Likewise, analysis of biopsy tissue from subjects with PD in the current study revealed higher CD3+ cell counts compared with HC subjects concurrent with an increased chemoattractant signals such as CCR5, which may account for the increased CD3+ T cells in the PD colon. Increased CD3+ T cells were also present in the colon of rotenone-treated mice. It is possible that the intestinal barrier dysfunction[8] and/or abnormal microbiota found in patients with PD[12 13 15 17 50–53] is promoting T-cell trafficking into the intestine. However, future studies with manipulation of intestinal microbiota are warranted to verify this effect.

More specific to our hypothesis, we showed, for the first time to the best of our knowledge, an upregulation of TLR4 mRNA and protein and TLR4 signalling with increased IRAK2/decreased TOLLIP as well as higher levels of TLR4-activated MyD88-dependent pathway mediated cytokines IL-1β, IFN-γ, IFN-β and CCL5 levels in colon mucosa of patients with PD. Interestingly, there was a robust correlation between markers of the TLR4 signalling and urinary sucralose suggesting that increased intestinal permeability could be a result of TLR4-mediated colonic inflammatory state.

To more directly demonstrate the pivotal role of TLR4 signalling in gut and brain inflammation and immune activation in PD, we used a rotenone mouse model of PD pathology and showed that TLR4-KO mice were protected against many of the PD-like consequences of rotenone-induced pathology. We and others have shown that oral rotenone-treated mice had increased number of CD3+ T cells and TLR4+ cells in the colonic mucosa and this pro-inflammatory state was associated with increased number of GFAP+ enteric glial cells and α-syn pathology in the colonic myenteric plexuses.[31 54 55] Taken together, these findings may suggest that intestinal inflammation leads to activation of enteric glial cells. Increased activation of enteric glial cells has also been reported in patients with PD.[56] In the current study, we found that loss of TLR4 significantly mitigated the effect of rotenone on intestinal barrier integrity, myenteric plexus GFAP expression, colonic α-syn, SN microglial activation and dopaminergic cell loss and motor function impairment. Our findings corroborate with the prior study that showed that knocking out TLR4 mitigates neuroinflammation in the brain.[57] Taken together, our findings in both human samples and a rodent model strongly suggest a possible role for TLR4-mediated signalling in gut leakiness, gut-derived inflammation, neuroinflammation and neurodegeneration in PD.

The observed TLR4-mediated immune activation in the colon and the brain in PD could be secondary to changes in the intestinal microbiota. Our findings support this notion and suggest that both rotenone treatment and loss of key bacterial recognition receptor, TLR4, resulted in a 'pro-inflammatory' dysbiotic microbiota compositions. For example, we found decreased F/B ratios and a reduction of the relative abundances of putative anti-inflammatory bacteria genera *Bifidobacterium* and/or *Lactobacillus,* and increased relative abundances of putative pro-inflammatory intestinal bacterial genera unclassified Rickenellaceae, *Allobaculum* and *Bacteroides* in WT-rotenone and/or TLR4-KO-vehicle mice. Our findings that loss of TLR4 receptor led to dysbiotic microbiota is not surprising and compatible with prior studies that showed loss of key mucosal immune molecules like TLR2, 5, NLRP3 resulted in pro-inflammatory dysbiotic microbiota compositions.[58 59] These studies suggest that there is a bi-directional interactive mechanism where the host's innate immune system (ie, TLR4, 2, 5 receptors and NLRP3) potentially shapes the microbiota's composition, and then the microbiota shapes the host's immune system leading to intestinal, systemic and neuroinflammation. Thus, it is intriguing to speculate that one reason that TLR4-KO could not completely protect rotenone-induced PD like pathology is that loss of TLR4 resulted in the pro-inflammatory dysbiotic microbiota. Further interventional studies like co-housing and stool transplantation, or gene silencing of TLR4 pathway is required to directly test this hypothesis and also to establish a direct link between TLR4, microbiota, intestinal and CNS inflammation and neurodegeneration in PD.

There are some limitation in our study. First, we acknowledge that our PD sample size is small. We elected to only study newly diagnosed patients with no constipation in order to avoid potential impact of constipation and long duration of disease on our outcomes measures. It is very difficult to recruit non-constipated patients with PD who are willing to undergo sigmoidoscopy and sigmoid biopsy. Importantly, even with a small sample size, we detected robust and significant differences in TLR4 and CD3 reactivity, barrier integrity disruption, pro-inflammatory gene profiles in the colon and faecal microbiota composition between subjects with PD and HC subjects. Even though there was no statistical difference between PD and controls, we also acknowledge the age differences in our cohort of patients with PD.

In summary, our proof-of-concept and translational study further support the notion that microbiota and gut-derived inflammatory processes are involved in neuroinflamamtion and neurodegeneration in PD and TLR4 signalling pathway, at least in part, mediate this interaction. Further interventional animal study is required to establish a direct causal link between TLR4 and PD pathology. Also, further human study using large PD cohort is required to confirm our finding which had a limited and small sample size. Nonetheless, our study suggests that TLR4 is a promising therapeutic target for PD and provides the scientific premise for future interventional studies.

Author affiliations
[1]Division of Pharmacology, Utrecht Institute for Pharmaceutical Sciences, Faculty of Science, Utrecht University, Utrecht, The Netherlands
[2]Department of Internal Medicine, Division of Digestive Disease and Nutrition, Rush University Medical Center, Chicago, Illinois, USA
[3]Sequencing Core Research Resources Center, University of Illinois at Chicago, Chicago, Illinois, USA
[4]Department of Biological Sciences, University of Illinois at Chicago, Chicago, Illinois, USA
[5]Department of of Neurology, Rush University Graduate College, Chicago, Illinois, USA
[6]Nutricia Research, Utrecht, The Netherlands

[7]Institute for Risk Assessment Sciences, Faculty of Veterinary Medicine, Utrecht University, Utrecht, The Netherlands

Contributors (1) Research project: A. Conception, B. Organisation, C. Execution; D. Supervision; (2) statistical analysis: A. Design, B. Execution, C. Review and Critique; (3) manuscript preparation: A. Writing of the first draft, B. Review and critique. PP-P: 1A, 1B, 1C, 2A, 2B, 3A, 3B. HBD: 1A, 1B, 1C, 2A, 2B, 3A, 3B. PAE: 1B, 1C, 2A, 2B, 2C, 3B. CBF: 1B, 1C, 1D, 2C, 3B. AMH: 1B, 1C, 2B, 3B. MS: 1B, 2C, 3B. RMV: 1B, 2C, 3B. JHK: 1B, 2C, 3B. KMS: 1B, 2C, 3B. JG: 1B, 2C, 3B. ADK: 1A, 1C, 1D, 2C, 3B. AK: 1A, 1C, 1D, 2C, 3B.

Funding The authors have not declared a specific grant for this research from any funding agency in the public, commercial or not-for-profit sectors.

Competing interests Professor Dr JG is an employee of Nutricia Research, Utrecht, The Netherlands. All other authors report no potential conflicts of interest.

Ethics approval Animal procedures were approved by the Ethical Committee of Animal Research of Utrecht University, The Netherlands.

Provenance and peer review Not commissioned; externally peer reviewed.

REFERENCES

1 Hirsch EC, Hunot S. Neuroinflammation in Parkinson's disease: a target for neuroprotection? *Lancet Neurol* 2009;8:382–97.
2 Hirsch EC, Vyas S, Hunot S. Neuroinflammation in Parkinson's disease. *Parkinsonism Relat Disord* 2012;18 Suppl 1(Suppl 1):S210–S212.
3 Xanthos DN, Sandkühler J. Neurogenic neuroinflammation: inflammatory CNS reactions in response to neuronal activity. *Nat Rev Neurosci* 2014;15:43–53.
4 Garcia-Esparcia P, Llorens F, Carmona M, *et al*. Complex deregulation and expression of cytokines and mediators of the immune response in Parkinson's disease brain is region dependent. *Brain Pathol* 2014;24:584–98.
5 Mogi M, Harada M, Narabayashi H, *et al*. Interleukin (IL)-1 beta, IL-2, IL-4, IL-6 and transforming growth factor-alpha levels are elevated in ventricular cerebrospinal fluid in juvenile parkinsonism and Parkinson's disease. *Neurosci Lett* 1996;211:13–16.
6 Brodacki B, Staszewski J, Toczyłowska B, *et al*. Serum interleukin (IL-2, IL-10, IL-6, IL-4), TNFalpha, and INFgamma concentrations are elevated in patients with atypical and idiopathic parkinsonism. *Neurosci Lett* 2008;441:158–62.
7 Reale M, Iarlori C, Thomas A, *et al*. Peripheral cytokines profile in Parkinson's disease. *Brain Behav Immun* 2009;23:55–63.
8 Forsyth CB, Shannon KM, Kordower JH, *et al*. Increased intestinal permeability correlates with sigmoid mucosa alpha-synuclein staining and endotoxin exposure markers in early Parkinson's disease. *PLoS One* 2011;6:e28032.
9 Keshavarzian A, Green SJ, Engen PA, *et al*. Colonic bacterial composition in Parkinson's disease. *Movement Disorders* 2015;30:1351–60.
10 Devos D, Lebouvier T, Lardeux B, *et al*. Colonic inflammation in Parkinson's disease. *Neurobiol Dis* 2013;50:42–8.
11 Tan AH, Mahadeva S, Thalha AM, *et al*. Small intestinal bacterial overgrowth in Parkinson's disease. *Parkinsonism Relat Disord* 2014;20:535–40.
12 Scheperjans F, Aho V, Pereira PAB, *et al*. Gut microbiota are related to Parkinson's disease and clinical phenotype. *Movement Disorders* 2015;30:350–8.
13 Unger MM, Spiegel J, Dillmann KU, *et al*. Short chain fatty acids and gut microbiota differ between patients with Parkinson's disease and age-matched controls. *Parkinsonism Relat Disord* 2016;32:66–72.
14 Helander HF, Fändriks L. Surface area of the digestive tract - revisited. *Scand J Gastroenterol* 2014;49:681–9.
15 Hopfner F, Künstner A, Müller SH, *et al*. Gut microbiota in Parkinson disease in a northern German cohort. *Brain Res* 2017;1667:41–5.
16 Petrov VA, Saltykova IV, Zhukova IA, *et al*. Analysis of Gut Microbiota in Patients with Parkinson's Disease. *Bull Exp Biol Med* 2017;162:734–7.
17 Bedarf JR, Hildebrand F, Coelho LP, *et al*. Functional implications of microbial and viral gut metagenome changes in early stage L-DOPA-naïve Parkinson's disease patients. *Genome Med* 2017;9:39.
18 Sampson TR, Debelius JW, Thron T, *et al*. Gut Microbiota Regulate Motor Deficits and Neuroinflammation in a Model of Parkinson's Disease. *Cell* 2016;167:1469–80.
19 Cryan JF, O'Mahony SM. The microbiome-gut-brain axis: from bowel to behavior. *Neurogastroenterology & Motility* 2011;23:187–92.
20 Lyte M. Microbial endocrinology in the microbiome-gut-brain axis: how bacterial production and utilization of neurochemicals influence behavior. *PLoS Pathog* 2013;9:e1003726.
21 Chen Y, Yu M, Liu X, *et al*. Clinical characteristics and peripheral T cell subsets in Parkinson's disease patients with constipation. *Int J Clin Exp Pathol* 2015;8:2495–504.
22 Braak H, Del Tredici K. Invited Article: Nervous system pathology in sporadic Parkinson disease. *Neurology* 2008;70:1916–25.
23 Shannon KM, Keshavarzian A, Dodiya HB, *et al*. Is alpha-synuclein in the colon a biomarker for premotor Parkinson's Disease? Evidence from 3 cases. *Movement Disorders* 2012;27:716–9.
24 Hilton D, Stephens M, Kirk L, *et al*. Accumulation of α-synuclein in the bowel of patients in the pre-clinical phase of Parkinson's disease. *Acta Neuropathol* 2014;127:235–41.
25 Stokholm MG, Danielsen EH, Hamilton-Dutoit SJ, *et al*. Pathological α-synuclein in gastrointestinal tissues from prodromal Parkinson disease patients. *Ann Neurol* 2016;79:940–9.
26 Guan J, Pavlovic D, Dalkie N, *et al*. Vascular Degeneration in Parkinson's Disease. *Brain Pathol* 2013;23:154–64.
27 Shaikh M, Rajan K, Forsyth CB, *et al*. Simultaneous gas-chromatographic urinary measurement of sugar probes to assess intestinal permeability: use of time course analysis to optimize its use to assess regional gut permeability. *Clin Chim Acta* 2015;442:24–32.
28 Pal GD, Shaikh M, Forsyth CB, *et al*. Abnormal lipopolysaccharide binding protein as marker of gastrointestinal inflammation in Parkinson disease. *Front Neurosci* 2015;9:306.
29 Engen PA, Dodiya HB, Naqib A, *et al*. The potential role of gut-derived inflammation in multiple system atrophy. *J Parkinsons Dis* 2017;7:331–46.
30 Voigt RM, Keshavarzian A, Losurdo J, *et al*. HIV-associated mucosal gene expression: region-specific alterations. *AIDS* 2015;29:537–46.
31 Perez-Pardo P, Dodiya HB, Broersen LM, *et al*. Gut-brain and brain-gut axis in Parkinson's disease models: Effects of a uridine and fish oil diet. *Nutr Neurosci* 2017 12.
32 Balda MS, Matter K. Tight junctions at a glance. *J Cell Sci* 2008;121:3677–82.
33 Poritz LS, Garver KI, Green C, *et al*. Loss of the tight junction protein ZO-1 in dextran sulfate sodium induced colitis. *J Surg Res* 2007;140:12–19.
34 Perez-Pardo P, Dodiya HB, Engen PA, *et al*. Gut bacterial composition in a mouse model of Parkinson's disease. *Benef Microbes* 2018;9:799–814.
35 Jankovic J, McDermott M, Carter J, *et al*. Variable expression of Parkinson's disease: a base-line analysis of the DATATOP cohort. The Parkinson Study Group. *Neurology* 1990;40:1529–34.
36 Goetz CG, Poewe W, Rascol O, *et al*. Movement disorder society task force report on the hoehn and yahr staging scale: Status and recommendations. *Mov Disord* 2004;19:1020–8.
37 Gutsmann T, Müller M, Carroll SF, *et al*. Dual role of lipopolysaccharide (LPS)-binding protein in neutralization of LPS and enhancement of LPS-induced activation of mononuclear cells. *Infect Immun* 2001;69:6942–50.
38 Wurfel MM, Kunitake ST, Lichenstein H, *et al*. Lipopolysaccharide (LPS)-binding protein is carried on lipoproteins and acts as a cofactor in the neutralization of LPS. *J Exp Med* 1994;180:1025–35.
39 Gegner JA, Ulevitch RJ, Tobias PS. Lipopolysaccharide (LPS) signal transduction and clearance. Dual roles for LPS binding protein and membrane CD14. *J Biol Chem* 1995;270:5320–5.
40 Erny D, Hrabě de Angelis AL, Jaitin D, *et al*. Host microbiota constantly control maturation and function of microglia in the CNS. *Nat Neurosci* 2015;18:965–77.
41 Fernandes J, Su W, Rahat-Rozenbloom S, *et al*. Adiposity, gut microbiota and faecal short chain fatty acids are linked in adult humans. *Nutr Diabetes* 2014;4:e121.
42 Deleidi M, Gasser T. The role of inflammation in sporadic and familial Parkinson's disease. *Cell Mol Life Sci* 2013;70:4259–73.
43 Dias V, Junn E, Mouradian MM. The role of oxidative stress in Parkinson's disease. *J Park Dis* 2013;3:461–91.
44 Glass CK, Saijo K, Winner B, *et al*. Mechanisms underlying inflammation in neurodegeneration. *Cell* 2010;140:918–34.
45 Luna E, Luk KC. Bent out of shape: α-Synuclein misfolding and the convergence of pathogenic pathways in Parkinson's disease. *FEBS Lett* 2015;589:3749–59.
46 Ransohoff RM. How neuroinflammation contributes to neurodegeneration. *Science* 2016;353:777–83.
47 Rea K, Dinan TG, Cryan JF. The microbiome: A key regulator of stress and neuroinflammation. *Neurobiol Stress* 2016;4:23–33.
48 Dinan TG, Cryan JF. Gut instincts: microbiota as a key regulator of brain development, ageing and neurodegeneration. *J Physiol* 2017;595:489–503.
49 Dinan TG, Cryan JF. Gut-brain axis in 2016: Brain-gut-microbiota axis - mood, metabolism and behaviour. *Nat Rev Gastroenterol Hepatol* 2017;14:69–70.
50 Hasegawa S, Goto S, Tsuji H, *et al*. Intestinal dysbiosis and lowered serum lipopolysaccharide-binding protein in parkinson's disease. *PLoS One* 2015;10:e0142164.
51 Hill-Burns EM, Debelius JW, Morton JT, *et al*. Parkinson's disease and Parkinson's disease medications have distinct signatures of the gut microbiome. *Movement Disorders* 2017;32:739–49.
52 Li W, Wu X, Hu X, *et al*. Structural changes of gut microbiota in Parkinson's disease and its correlation with clinical features. *Sci China Life Sci* 2017;60:1223–33.
53 Petrov VA, Saltykova IV, Zhukova IA, *et al*. Analysis of gut microbiota in patients with parkinson's disease. *Bull Exp Biol Med* 2017;162:734–7.

54 Pan-Montojo F, Anichtchik O, Dening Y, *et al*. Progression of Parkinson's disease pathology is reproduced by intragastric administration of rotenone in mice. *PLoS One* 2010;5:e8762.
55 Drolet RE, Cannon JR, Montero L, *et al*. Chronic rotenone exposure reproduces Parkinson's disease gastrointestinal neuropathology. *Neurobiol Dis* 2009;36:96–102.
56 Clairembault T, Leclair-Visonneau L, Neunlist M, *et al*. Enteric glial cells: New players in Parkinson's disease? *Movement Disorders* 2015;30:494–8.
57 Maes M, Kubera M, Leunis JC. The gut-brain barrier in major depression: intestinal mucosal dysfunction with an increased translocation of LPS from gram negative enterobacteria (leaky gut) plays a role in the inflammatory pathophysiology of depression. *Neuro Endocrinol Lett* 2008;29:117–24.
58 Henao-Mejia J, Elinav E, Jin C, *et al*. Inflammasome-mediated dysbiosis regulates progression of NAFLD and obesity. *Nature* 2012;482:179–85.
59 Jin C, Henao-Mejia J, Flavell RA. Innate immune receptors: key regulators of metabolic disease progression. *Cell Metab* 2013;17:873–82.